Journal of Cell Science 108, 685-698 (1995)
Printed in Great Britain © The Company of Biologists Limited 1995

Identification of a novel Ca^{2+}-regulated protein that is associated with the marginal band and centrosomes of chicken erythrocytes

Jian Zhu[1], Stephen E. Bloom[2], Elias Lazarides[1,*] and Catherine Woods[1,†]

[1]Department of Pharmacology, Merck Research Laboratories, West Point, PA 19486, USA
[2]Department of Avian and Aquatic Animal Medicine, Cornell University, Ithaca, NY 14853-5601, USA

*Present address: Astral Inc., 3040 Science Park Rd, San Diego, CA 92121, USA
†Author for correspondence at present address: Alliance Pharmaceuticals Co., 3040 Science Park Rd, San Diego, CA 92121, USA

SUMMARY

We have identified a novel Ca^{2+}-regulated protein, p23, that is expressed specifically in avian erythrocyte and thrombocyte lineages. Sequence analysis of this 23 kDa protein reveals that it bears no homology to any known sequence. In mature definitive erythrocytes p23 exists in equilibrium between a soluble and a cytoskeletal bound pool. The cytoskeletal fraction is associated with the marginal band of microtubules, centrosomes and nuclear membrane under conditions of low free $[Ca^{2+}]$. An increase in free $[Ca^{2+}]$ to10^{-6} M is sufficient to induce dissociation of >95% of bound p23 from its target cytoskeletal binding sites, yet this $[Ca^{2+}]$ has little effect on calmodulin-mediated MB depolymerization. Analysis of p23 expression and localization during erythropoiesis together with results from heterologous p23 expression in tissue cultured cells demonstrates that this protein does not behave as a bone fide microtubule-associated protein. In addition, the developmental analysis revealed that although p23 is expressed early in definitive erythropoeisis, its association with the MB, centrosome and nuclear membrane occurs only in the final stages of differentiation. This cytoskeletal association correlates with marked p23 stabilization and accumulation at a time p23 expression is being markedly downregulated. We hypothesize that the mechanism of p23 association to the MB and centrosomes may be induced in part by a decrease in intracellular $[Ca^{2+}]$ during the terminal stages of definitive erythropoiesis.

Key words: calcium-regulated, chick erythrocyte, centrosome, marginal band

INTRODUCTION

Microtubules (MTs) are a major class of structural filaments, which play a key role in a wide repertoire of cellular events: mitosis and meiosis, ordered vesicle transport, intracellular organization of Golgi and lysosomal vesicles, and cell shape and motility, to name but a few (for reviews see: Dustin, 1984; Kirschner and Mitchison, 1986). MTs exhibit an inherent property of dynamic instability both in vitro (Mitchison and Kirschner, 1984a,b; Horio and Hotani, 1986) and in vivo (Cassimeris et al., 1988; Schulze and Kirschner, 1988) and it is this property that is pivotal for plasticity in cellular MT organization and function. However, highly stable MT configurations exist within some terminally differentiated cell types such as axonal processes of neurons (Baas and Black, 1990; Baas and Ahmad, 1992; Reinsch et al., 1991), polarized epithelial cells (Bré et al., 1990; Wacker et al., 1992), myocytes (Tassin et al., 1985) and platelets (Kenney and Linck, 1985; Kowit et al., 1988) and the nucleated erythrocytes of nonmammalian vertebrates (Behnke, 1970; Murphy et al., 1986). While considerable effort has been directed towards the elucidation of the mechanism and functional significance of dynamic instability, the mechanisms underlying the conversion of these normally dynamic MT structures into highly ordered arrays remain less well defined. MT-associated proteins (MAPs) have been shown to induce profound changes in MT form and function (for revue see Olmsted, 1986) but how they are recruited during differentiation for an orderly transition in MT morphology and function is poorly understood.

The marginal band of MTs (MB) provides a relatively simple system to study the morphogenesis of stable MT arrays. MBs are found in nucleated nonmammalian erythrocytes and thrombocytes as well as mammalian platelets. They consist of a highly ordered, stable MT bundle that underlies the plasma membrane at the equatorial plane of the cell (Behnke, 1970; Barrett and Dawson, 1974; Cohen, 1978). The MB helps confer and maintain the elliptical shape of these cells as well as being an aid in resisting the deformation forces experienced during circulation (Barret and Dawson, 1974; Joseph-Silverstein and Cohen, 1984). Several studies have been undertaken to understand how the strict temporal and spatial regulation of the biogenesis of this structure is achieved during erythropoiesis. The predominant β-tubulin isoform in mature avian erythrocytes, cβ6 (Murphy and Wallis, 1983a; Murphy et al., 1987), exhibits properties in vitro that are consistent with a more stable polymeric pool in vivo. It exhibits a lower critical concentration for polymerization and a tendency to form fewer but longer and more stable MTs compared to brain β-tubulin,

and is specifically expressed in terminally differentiating erythroid cells (Murphy and Wallis, 1983b, 1985, 1986). The presence of the MT bundling MAPs, MAP2, tau and syncolin in MBs (Murphy and Wallis, 1985; Feick et al., 1991) suggests that the regulated expression of these proteins during erythropoeisis would both induce bundling and increase MT stability. Reconstitution experiments have indicated that spatial regulation, limiting MB formation to a single band at the equatorial rim of the cell, is determined by specifically localized membrane binding sites (Miller and Solomon, 1984; Swan and Solomon; 1984). Although several candidate polypeptides have been described on the basis that they colocalize to the MB site independently of an intact MB-MT bundle (Birgbauer and Solomon, 1989; Stetzkowski-Marden et al., 1991), the exact molecular nature of the interaction between the MB and cytoplasmic face of the membrane remains ill-defined.

A key issue in MB biogenesis concerns whether MT-MB nucleation occurs from the centrosome or localized MT-nucleating activity at the membrane. In most vertebrate cells the centrosome serves as the major MT organizing center (MTOC; Pickett-Heaps, 1969; Brinkley, 1985; Mazia, 1987; Kimble and Kariyama, 1992), which determines the precise arrangement and dynamics of cytoplasmic MT arrays. MTOCs dramatically lower the critical tubulin concentration required for polymer nucleation and can dictate the orientation, protofilament composition and number of MTs emanating out from them (Brenner and Brinkley, 1982; Mitchison and Kirschner, 1984a). Centrosomes typically consist of a pair of centrioles connected by a system of Ca^{2+}-activated filaments, with the parental centriole being surrounded by a cloud of diffuse pericentriolar material or centrosomal matrix (PCM; Gould and Borisy, 1977). It is this material that contains the MT nucleation sites which can persist (be regenerated) in cells from which centrioles have been microsurgically removed (Maniotis and Schliwa, 1991). PCM-associated components reported to play a key role in MT nucleating activity include γ-tubulin (Oakley and Oakley, 1989; Oakley et al., 1991; Joshi et al., 1992; Félix et al., 1994; Stearns et al., 1994) and a 51 kDa GTP/ITP-binding protein (Sakai and Ohta, 1991). Gain of PCM-directed MT nucleating activity has been correlated with recruitment of dispersed γ-tubulin to the PCM (Félix et al., 1994; Stearns et al., 1994) whereas cell-cycle-dependent dissociation and reassociation of the PCM-1 antigen with the centrosome correlates with changes in centrosomal MT activity at the onset and end of mitosis, respectively (Balczon et al., 1994). Erythroid differentiation, in common with many other post-mitotic differentiated cell types entails a dramatic switch from the centrosomally directed orchestration of MT arrays as a function of the cell cycle into the elaboration of a more rigid, stable MT structure, which frequently does not appear to be associated with centrosomal structures (Tassin et al. 1985; Mogensen and Tucker, 1987; Tucker et al., 1992; Euteneuer et al., 1985). Rather, in some of these other cell types, it has been shown that dispersed PCM nucleates formation of these MT structures (Tucker et al., 1992; Tassin et al., 1985). It remains to be seen if the MB arises from localized PCM at the membrane or whether the bundled MTs interact with the membrane after formation through prelocalized membrane binding sites, and which specific PCM antigens implicated in MT-nucleating activity may be involved in these interactions.

We report here the identification and characterization of a new calcium-regulated protein of 23 kDa, p23, that is expressed specifically in avian erythrocytes and thrombocytes. This protein exists in equilibrium in soluble and cytoskeletally bound pools in a Ca^{2+}-dependent manner. The cytoskeletal fraction localizes to the MB, the centrosomes and the nuclear membrane of mature erythrocytes in the presence of low free cytoplasmic Ca^{2+}. As the free Ca^{2+} levels approach 10^{-6} M, p23 dissociates from these structures and becomes diffusely localized in the cytoplasm. It exhibits a Ca^{2+}-dependent shift under SDS-PAGE, a characteristic of Ca^{2+}-binding proteins. Analysis of the full-length cDNA sequence reveals no homology with any known sequence; in particular it shares no homology with any of the known MAPs. Furthermore, it lacks any conventional consensus sequence for the EF hand Ca^{2+}-binding domain (Kretsinger, 1980; Nakayama et al., 1992) or the ~70 amino acid stretch of repeat structures encoding the Ca^{2+}-binding site of the annexin family (Burgoyne and Geisow, 1989). Detailed analysis of p23 expression and localization during erythropoiesis with respect to the development of the MB and the progression through terminal differentiation indicate that its association with both the MB and centrosomes occurs during the final tailoring step of these two structures as the cells become postmitotic. We speculate that this protein may play a regulatory role in a Ca^{2+}-dependent manner in establishing the extreme stability of these structures in the mature erythrocyte.

MATERIALS AND METHODS

Materials

Anti-p23 monoclonal antibodies were generated as described (Woods et al., 1995, accompanying paper). Anti-chick cβ6 erythrocyte tubulin rabbit antisera was generously provided by D. Murphy (Department of Cell Biology and Anatomy, Johns Hopkins University School of Medicine) and anti-human centrosomal antisera by W. Brinkley (Department of Cell Biology, University of Alabama in Birmingham). Anti-chicken β-spectrin rabbit antisera has been characterized previously (Nelson and Lazarides, 1983). The following were obtained commercially: β-actin probe (Clontech); mouse monoclonal anti-β-tubulin IgG (Amersham); fertilized chicken eggs (SPAFAS); Sephacryl-200, CNBr-activated Sepharose-4B, ProRPC HR5/10, FPLC, oligo(dT)-cellulose spin column, QuickPrep mRNA purification, pSVL (Pharmacia, LKB); λEHlox™ vector (Novagen); endoproteinases (Boehringer Mannheim, Promega); Zeta-Probe nylon membrane (Bio-Rad); α-MEM, Lipofectin, Superscript RT (Gibco); alkaline phosphatase-, fluorescein- and rhodamine-conjugated secondary antibodies (Cappel, Boehringer Mannheim); pCDNA1, pRC/RSV (Invitrogen); Decaprime random primer labelling (Ambion); calcium ionophore A23187, nocodazole, GTP (Sigma).

Cell preparation

Mature chicken red blood cells (RBCs) and erythroid cells from 5- to 18-day embryos were collected as previously described (Blikstadt and Lazarides, 1983). Erythroblasts were isolated from 2- to 4-day chick embryos into α-MEM by first teasing the blood islands of isolated blastodiscs and further dispersing them with an 18-gauge needle. The cell suspension was filtered through a 70 μm cell strainer (Falcon) and the cell suspension overlaid on a Percoll cushion (density 1.065 g ml^{-1}) to remove yolk and debris. After centrifugation at 800 ***g*** for 10 minutes, the cell pellet was resuspended in αMEM. Bone marrow was expelled from the tibia of 1- to 7-day-old chicks into αMEM medium containing 1 mM GTP, gently dispersed through an 18-gauge needle, and the suspension was filtered through a cell strainer. Chicken

embryo fibroblast (CEF) primary cultures were made from the muscle mass of 10- to 11-day chick embryos.

p23 purification and characterization

Chick p23 was purified from erythrocyte hypotonic lysates as described (Woods et al., 1995, accompanying paper). The FPLC-ProRPC step yielded 99% pure p23. Amino acid compositional analysis and peptide sequence analysis were carried out as described for turkey p23 (see accompanying paper by Woods et al.). Rabbit polyclonal antibodies against chick p23 were generated using FPLC-purified p23. The polyclonal antibody was then affinity-purified from rabbit serum using purified p23 coupled to Sepharose 4B.

cDNA cloning, sequencing and 5′ RACE

An expression cDNA library was constructed in λ-EHlox™ vector from poly(A)$^+$ RNA isolated from erythrocytes of 8 day chick embryos. Mixed cocktails of monoclonal antibodies at 1:50 dilution were used to screen the 1×10^6 plaques; 28 positive clones were plaque purified to homogenity and auto-subcloned into pEXlox. The sequence (16-1461) was determined by dideoxy sequencing of all the clones. The 5′ non-coding region (1-16) was cloned by 5′ RACE (Loh, 1991). First strand cDNA was primed using a p23 gene-specific antisense oligonucleotide p23-GSP1 ([323-339]: 5′-ACG CCG TGC TCC TTC AT-3′), the tailed cDNA was then amplified by a nested p23-GSP2 ([123-139]: 5′-AGC GCC GGG TTC CGA ACC-3′). The fragment was then blunt-end ligated into pBluescript-KS and sequenced.

Northern and western blot analyses

Total RNA was isolated by homogenizing perfused tissues in guanidium isothiocyanate and pelleting through cesium chloride. Poly(A)$^+$ RNA was then isolated using oligo(dT)-cellulose spun columns. Poly(A)$^+$RNA from cultured cells and erythroid cells was isolated by directly passing the guanidium isothiocyanate lysate over an oligo(dT) spun column by the QuickPrep mRNA purification protocol (Pharmacia). For northern analysis, RNA was fractionated on a 1% agarose gel containing 2.2 M formaldehyde and capillary blotted onto Zeta-Probe GT nylon membrane. The blot was UV cross-linked, baked for 1 hour at 80°C and hybridized with ^{32}P-radiolabeled probes at 65°C for 18 hours in 0.25 M Na_2HPO_4, pH 7.2, 7% SDS. The blot was then washed twice in 20 mM Na_2HPO_4, 5% SDS and twice in 20 mM Na_2HPO_4, 1% SDS before being exposed to film. For reprobing, the blots were stripped with 0.1×SSC, 0.5% SDS for 20 minutes at 95°C before being rehybridized with a second probe. Two probes were used: (a) the reading frame of p23, generated from the p23 clone in pEXlox by PCR using the two primers: p23-MET-5 (5′-ATG GAT CGC GAT CGG AT-3′) and p23-TGA-3 (5′-TCA GCC GTA GTG CCC GC-3′); (b) a PCR-derived fragment of chicken erythrocyte β-tubulin (cβ6) cDNA (Murphy et al., 1987). Two primers were derived from regions of the cβ6 gene that are least conserved compared with other tubulins: cβ6 sense (5′-GAT ATT GCC GGA AAC TAC TGT-3′) and cβ6 antisense (5′-GAG GAT GGC ATT ATA GGG C-3′). First strand cDNA was synthesized by poly(A)$^+$RNA from bone marrow using SuperscriptRT and then was used as template for PCR. The PCR fragments were agarose gel purified by electroelution, and radiolabeled by Decaprime™ random primer labeling.

For western analysis, perfused chick tissue lysates (lysis buffer: 50 mM Tris-HCl, pH 7.8, 50 mM NaCl, 1% SDS, 0.5% Triton, 100 μg/ml PMSF, 1 unit/ml aprotinin, 10 μg/ml leupeptin, 1 mM Na_3N) were separated by 20% SDS-PAGE and processed for western blot analysis as described (Woods et al., 1995, accompanying paper). To study calcium effects on p23 electrophoretic mobility under SDS-PAGE, 1 mM $CaCl_2$ or 1 mM EGTA was included in the sample buffer, running buffer and SDS-gel as described (Burgess et al., 1980).

Immunofluorescence

Immunofluorescence (IF) was performed essentially as previously described (Granger and Lazarides, 1982) with the following modifications. After allowing cells to settle onto coverslips in αMEM (cultured cells were grown on coverslips), adherent cells were fixed in 2% formaldehyde in TBS and permeabilized with 0.5% Triton X-100 in TBS for 5 minutes. Cells were incubated in primary antibody in TBS+ 2% goat serum for 1 hour at 37°C, rinsed in TBS, then TBS + 10% goat serum prior to incubation with fluorescein-conjugated or rhodamine-conjugated secondary antibodies. The coverslips were mounted in VectorShield™ and visualized with a Zeiss Axiophot microscope using a 63× or 100× lens. For modulation of cytoplasmic $[Ca^{2+}]_{free}$, adherent mature chicken erythrocytes in PIPES buffer (100 mM PIPES, pH 6.94, 1 mM $MgCl_2$, 1 mM EGTA, 1 mM ATP) were equilibrated with different free $[Ca^{2+}]$ using Ca^{2+}/EGTA buffers as described (Cande, 1980) in the presence of the calcium ionophore A23187 (5 μM) at 38°C. Cells were fixed after appropriate time intervals and processed for IF.

Construction of expression vectors and transient expression studies

The reading frame of p23 gene from pEXlox was first subcloned into the adaptor vector CLA 12 NCO (Hughes et al., 1987) to ensure an authentic initiator ATG for p23. The *Cla*I-*Hin*dIII fragment was then subcloned into pSVL, pCDNAI and pRC/RSV vectors. Double $CsCl_2$-banded DNA was introduced into COS, 3T3, and CEF cells by Lipofection or calcium phosphate-mediated transfection. Expression of p23 was monitored by western blotting and IF staining 24 to 72 hours after transfection.

RESULTS

Molecular characterization of p23

The mAbs raised against the turkey p23 antigen reacted with a single polypeptide in chick erythrocyte lysates of M_r 23,000, from here on designated chick p23 (Fig. 1A), whose expression appeared to be restricted to the erythroid lineage (Fig. 1B). Western blot analysis of the buffy coat layer, purified macrophages and lymphocytes indicated that it was not even present in these other hematopoietic cell types (data not shown).

These anti-p23 mAbs identified 28 positive plaques with insert sizes ranging from 1.2 kb to 1.46 kb in the chick erythroblast λEHlox expression library. Sequencing yielded the nucleotide sequence from 16 to 1461 of the full-length sequence for p23 shown in Fig. 2. The 5′ non-coding region (1-16) was cloned and sequenced by 5′ RACE. The 39, 20, 53 and 9 amino acid length peptide sequences (58% of the predicted sequence) obtained by direct peptide sequencing of the RPC-purified p23 (99% pure after this step) are denoted by the heavy lines under the peptide sequence designated by the cDNA sequence shown in Fig. 2. They show an exact match with the sequence encoded by the full-length cDNA sequence, confirming the identity of the clones. In addition, the amino acid composition calculated from the predicted protein sequence exactly matched that obtained directly from amino acid compositional analysis of the purified protein (data not shown). Taken together, these data provide firm evidence that this sequence represents that of the p23 polypeptide recognized by the antibodies. The sequence encodes a basic protein, which is consistent with the basic pI of ≈9.5 observed by isoelectric focusing of the purified erythrocyte protein (data not shown).

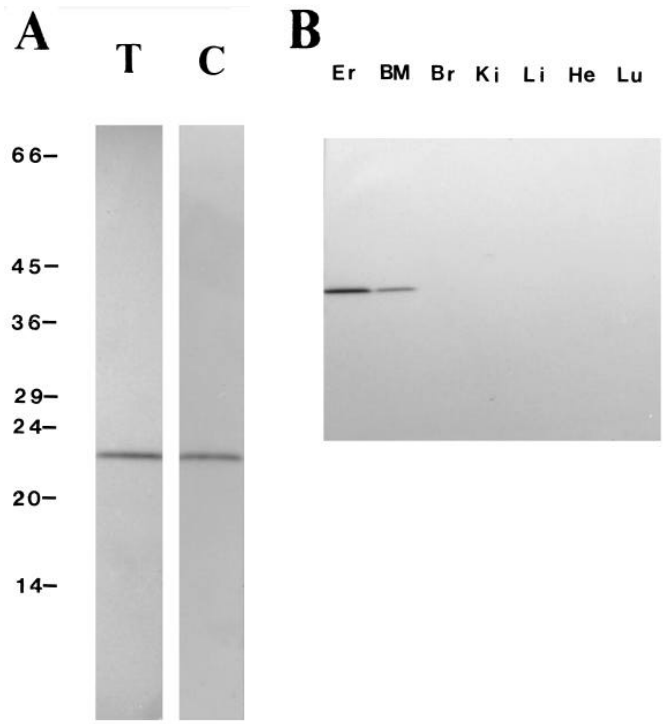

Fig. 1. Western blot analysis. (A) Turkey (T) and chicken (C) erythrocyte lysates separated by 20% SDS-PAGE before being transferred to nitrocellulose and probed with the anti-turkey p23 mAb, 20E12B1. (B) Western blot analysis of perfused tissue lysates compared with erythrocyte and bone marrow cell lysates; 50 μg total protein was loaded per lane. The blot was probed with rabbit polyclonal anti-chick p23. Er, erythrocyte; BM, bone marrow; Br, brain; Ki, kidney; Li, liver; He, heart; Lu, lung.

The predicted relative molecular mass is 22,099, which corresponds well to the observed M_r of 23,000 by SDS-PAGE (Fig. 1). The sequence shares a high degree of homology with the normal turkey homologue (see accompanying paper by Woods et al.) but lacks homology with any previously sequenced protein in the Wisconsin GCG database.

Northern blot analysis of poly(A)$^+$ RNA isolated from different tissues of perfused chicks was performed to determine the transcript size and tissue specificity of p23 expression. As shown in Fig. 3A, a 1.6 kb band appeared in bone marrow RNA after a short exposure time (6 hours). This corresponded in size and intensity to the signal observed in RNA isolated from erythroblasts from chick embryos (data not shown). After one week of exposure, a faint 1.6 kb band was observed in RNA from brain, kidney and liver with a slightly stronger band in lung RNA. Probing the same blot with a β-actin probe (Fig. 3B) confirmed that these differences were not due to differential loadings of RNA but reflected a true difference in the steady-state levels of p23 transcripts between these different cells and tissues.

Southern blot analysis was performed using the full coding region of p23 as the probe. A single band was detected in *Hin*dIII digests but with *Eco*RI one major and two minor bands were also detected (data not shown). These results suggest that although a major single gene exists, p23 may be part of a multigene family.

p23 associates with the centrosomes, nuclear membrane and marginal band in chick erythrocytes and thrombocytes

To analyze the cellular distribution of p23, circulating adult chick erythrocytes were attached to coverslips and processed for IF. p23 antibodies were found to localize to the MB, cen-

```
TGGTGTTGCACGACGGCGGCGATGGATCGCGATCGGATCGTGGCGCTGTTCGGGGCCACCGGGAGGAGCGGCCGGGAGGCGCTGCGGAGG 90
                  M  D  R  D  R  I  V  A  L  F  G  A  T  G  R  S  G  R  E  A  L  R  R   23

GCGCTGCGGGAGGGCTACGCGGTATCGGCTCTGGTTCGGAACCCGGCGCTGCTGCCGCCCGACGCCGCGCCGTGCCGGGTGGTCCGCGGG 180
A  L  R  E  G  Y  A  V  S  A  L  V  R  N  P  A  L  L  P  P  D  A  A  P  C  R  V  V  R  G   53

GACGCGCTGCGCGCCGCCGACGTCAGCGCCACCGTGCGGGGGCAGCGCGCCGTCATCGTCACGTTGGGAACGCGCGGAGACATCGGTCCC 270
D  A  L  R  A  A  D  V  S  A  T  V  R  G  Q  R  A  V  I  V  T  L  G  T  R  G  D  I  G  P   83

ACCACCGTCCTATCAGACAGCACCCGCAACATCGTGGCCGCCATGAAGGAGCACGGCGTGCGCAAAGTGGTGGCGTGTCTGTCCGCCTTC 360
T  T  V  L  S  D  S  T  R  N  I  V  A  A  M  K  E  H  G  V  R  K  V  V  A  C  L  S  A  F   113

CTCTTATGGGATCCTGAGAAGGTCCCCACGCGGCTGCGGGCGCTGACGGAGGACCACGCGCGGATGCACGCCGTGCTGAGCGGGGCCGGG 450
L  L  W  D  P  E  K  V  P  T  R  L  R  A  L  T  E  D  H  A  R  M  H  A  V  L  S  G  A  G   143

CTGGATTACGTGGCCGTCATGCCGCCCCACATCGCCGACGACAAGCCGCTGACGGAGGCATACGAGGTCACGGTCGGTGGCACCGGCGGT 540
L  D  Y  V  A  V  M  P  P  H  I  A  D  D  K  P  L  T  E  A  Y  E  V  T  V  G  G  T  G  G   173

GGCTCGCGGGTCATCTCCACGCCGGACCTGGCCCATTTCCTCGTGCGCTGCCTCAGCACCACCGCGTTCGACGGGAAGAGCGTCTACGTC 630
G  S  R  V  I  S  T  P  D  L  A  H  F  L  V  R  C  L  S  T  T  A  F  D  G  K  S  V  Y  V   203

TGCGGGCACTACGGCTGAGGGGGGGCAGCGGGGGGCATGGGGGGCAGTGGGGGCATGGGGGGCAGTGGGGGCAGTGGGGTCAATAGGGAC 720
C  G  H  Y  G  *                                                                           208

ATTGAGGTCATTGGGGATATTGGGGTCAATGAGGGCAATGGGGGCAGTGGGGGCAATAGGGACATTGAGGTCATTGGGGGCATTGGGGTC 810
AATGAGGGCATTGGGGGCATTGGGGTCAATGGGGGCAATGGAGGCAGTGGGGGCATTGGGACACATGGGGACATGGGGGACATTGCGGTC 900
AATGGGGACATTGGGGGCAATGGAGGCAATGGGGATATGGGGGGCAATGGGGGCAGTGGGGACATGGGGGTCAATGGGGACATGGGAGGC 990
AATGGGGGCAATGGGGACATTGGGGGCATTGGGGGCAATGGGGACATTGGGGGCAATGGAGGCAATGGGGACATTGGGGTCAATGGGGTC 1080
AATGGGGACAATGGGGCCAATGGGGTCAGTGACACATTGGGGCCTTAGGGGTCAATGGGGACACTGGGGCCAATGGGGACACATTGTGGC 1170
CAATGGGGTCAATGGGGACATTGGGGTCAATGGGGACACATTGGGGCCAATGGGGTCAATGTGGACATTGGAGTCAATGGGGACATTGGG 1260
GCCAATGGGTTCAATGGGGACACAATGGGGCCAATGGGGACATAATGGGGCCAATGGGGTCAGTGGGGCCAATGGGGTGCAGATGTGGAC 1350
CCAAAATGGCGTAGATTTGACCCCAAAAAAGCCCCCACTTTTCCCCCCCCCCGAATCCCAACGCGGCCGTCGGTGATAAACTTCAATAAG 1440
GCCGAAAAAAAAAAAAAAAAA                                                                      1461
```

Fig. 2. p23 Peptide and cDNA sequences. The nucleotide sequence between 16 and 1461 was sequenced directly from positive clones isolated from the chick erythroblast λEXlox library. Nucleotide sequence 1-16 was obtained by 5′ RACE. The underlined stretches of the amino acid sequence predicted from the cDNA denote the sequences obtained by direct sequencing of the purified p23 protein. An exact match is seen between the observed and predicted sequence for these polypeptide stretches. This sequence is filed with GenBank under accession number L11171.

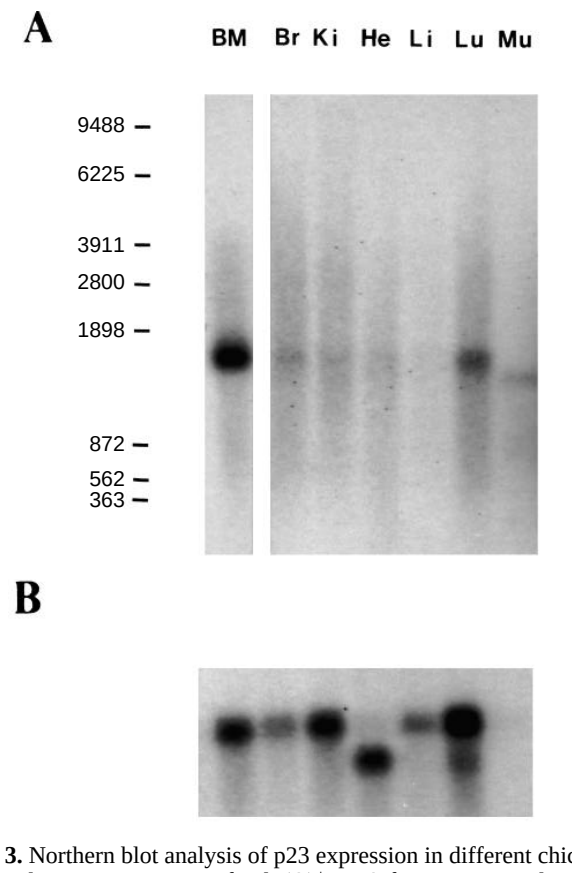

Fig. 3. Northern blot analysis of p23 expression in different chick cell and tissue types. 1 μg of poly(A)$^+$ RNA from tissues isolated from perfused chicks was separated by formaldehyde gel electrophoresis and probed with the full-length reading frame of p23 (A). The same blot was reprobed with a β-actin probe as a control (B). The tissues include bone marrow (BM), brain (Br), kidney (Ki), heart (He), liver (Li), lung (Lu) and muscle (Mu). The exposure time shown for the BM lane in A is 6 hours, whereas that for the remaining lanes is 6 days. The exposure time for the β-actin blot is 30 minutes. Note that cardiac tissue contains the cross-reactive γ-actin species but muscle actin does not cross-react with this β-actin probe.

trosomes and nuclear membrane (Fig. 4A,B). Cold methanol fixation/permeablization gives poor images with red cells because of the high hemoglobin content but limits the loss of small cytosolic polypeptides compared to Triton permeabilization. This is evidenced by the efficient retention of hemoglobin. Under these fixation conditions, a high content of diffuse cytosolic p23 reactivity was also observed (data not shown). This suggests that p23 exists in equilibrium in both insoluble and soluble form. Very brightly staining cells were occasionally observed (indicated by a T in Fig. 4A,B), which proved to be thrombocytes, the nonmammalian equivalent of platelets (Spurling, 1981). Indeed, if great care was not taken during handling of the blood prior to fixation to inhibit the clotting, these very bright cells appeared in aggregates (see also Fig. 3 of Murphy et al., 1986). The p23 antibodies reacted diffusely throughout the cytoplasm and also at the erythrocyte equatorial rim, i.e. at the MB. It should be noted that the exposure times in the images shown in Fig. 4 were adjusted to give optimal erythrocyte images, hence thrombocytes appear overexposed. With shorter exposure times the p23 MB localization in thrombocytes could be clearly seen. Interestingly, thrombocytes and platelets are thought to be developmentally related to the erythroid lineage (Lucas and Jamroz, 1961) and are the only other cell types known to express a MB of MTs. They also are the only other hematopoietic cell type besides erythrocytes to express p23 as shown by IF of bone marrow smears (data not shown). The p23 localization at the MB was confirmed by double IF using either antibodies against general β-tubulin or cβ6-tubulin (Murphy and Wallis, 1983a; Murphy et al., 1986). The centrosomal localization of p23 was confirmed by double IF using human autosomal anti-centrosomal antisera together with anti-p23 mAbs. The two dots revealed by anti-p23 to be juxtaposed to the the nucleus, generally at the long axis poles, also reacted with anti-centrosomal antisera (Fig. 4D).

Previously, the distinction between MB-associated proteins that might serve as potential MAPs compared to potential binding sites at the membrane has been made by determining if their localization was dependent on the integrity of the core MT bundle (Feick et al., 1991; Birgbauer and Solomon, 1989: Stetzkowski-Marden et al., 1991). Therefore, we analyzed the effect of destabilizing the MB using a combined treatment of cold (4°C) and the MT-destabilizing drug, nocodazole on p23 localization in the hope that this would give some insight into the potential functional role of p23. Pretreatment of the cells at 4°C for 1 hour prior to fixation completely depolymerized the microtubules of the MB, as evidenced by the lack of any MB staining with anti-tubulin mAb (Fig. 5A; see also Miller and Solomon, 1984), and also abolished the MB staining by anti-p23 antisera. Subsequent rewarming of the cells prior to fixation resulted in the re-formation of the MB of microtubules and the restoration of MB staining of p23, but the presence of nocodazole during rewarming inhibited both MT and p23 relocalization to the original MB site at the equatorial rim of the cell (Fig. 5B and C). In contrast, centrosomal and nuclear membrane localization of p23 was unaffected by all these treatments.

p23 is a Ca^{2+}regulated protein which is modulated by Ca^{2+} in vivo

To test the Ca^{2+}-sensitivity of chick p23, chick erythrocyte lysates underwent SDS-PAGE in the presence of either 1 mM Ca^{2+} or 1 mM EGTA followed by western blot analysis. This revealed that whereas on regular or EGTA-containing gels, p23 migrated with an apparent M_r of 23,000, in Ca^{2+}-containing gels there was a shift to an apparent M_r of ≈20,000 (Fig. 6A). We attempted to verify that p23 is a Ca^{2+}-binding protein by equilibrium dialysis. However, we were unable to purify sufficient quantities at high enough concentrations to obtain significant specific $^{45}Ca^{2+}$ binding data, since in our hands, even with calmodulin, we required concentrations of at least 200 μg/ml.

Ca^{2+} was found to also modulate whether p23 exists in soluble form or is associated with the cytoskeleton. When cells were lysed in the presence of EGTA-containing buffer, approximately 50% of p23 was found to be soluble and 50% remained with the insoluble cytoskeletal fraction (Fig. 6B.1). In contrast, in the presence of 1 mM Ca^{2+} more than 95% of p23 was soluble (Fig. 6B.2). To analyze this effect in greater detail, erythrocyte intracellular $[Ca^{2+}]_{free}$ was modulated by exposing the cells to different Ca^{2+}/EGTA buffers in the presence of the Ca^{2+} ionophore, A23187 at 38°C prior to fixation and processing for

IF. As shown in Fig. 7A and B, at low $[Ca^{2+}]_{free}$ ($\leq 10^{-8}$), anti-p23 and anti-tubulin staining showed the same pattern observed in nontreated erythrocytes fixed directly after isolation. When the $[Ca^{2+}]_{free}$ was increased to 10^{-6} M the staining of p23 at the centrosomes, nuclear membrane and MB became much weaker (Fig. 7C). Noticeably, at this $[Ca^{2+}]$ the MB MTs remained intact as evidenced by anti-β-tubulin staining (Fig. 7D). This strongly suggests that Ca^{2+}-induced p23 dissociation from the MB occurs before free Ca^{2+} levels reach concentrations that affect the core MT bundle of the MB. In cells exposed to free Ca^{2+} levels of 10^{-4} M, no p23 or tubulin staining was observed (Fig. 7E,F). (Note that with the fixation/permeabilization conditions used, much of the freely soluble proteins were washed away.) Thus at these high levels of cytosolic free Ca^{2+}, p23 becomes completely soluble and the MB fully disassembled. To test the reversibility of these Ca^{2+} effects, cells were exposed to 10^{-6} M to 10^{-4} M $[Ca^{2+}]_{free}$ in the presence of A23187 and then restored to Ca^{2+}-free EGTA buffer for 20 minutes (all at 38°C) prior to fixation. In cells that had been pre-exposed to 10^{-6} M $[Ca^{2+}]_{free}$, the MB and centrosomal localization of p23

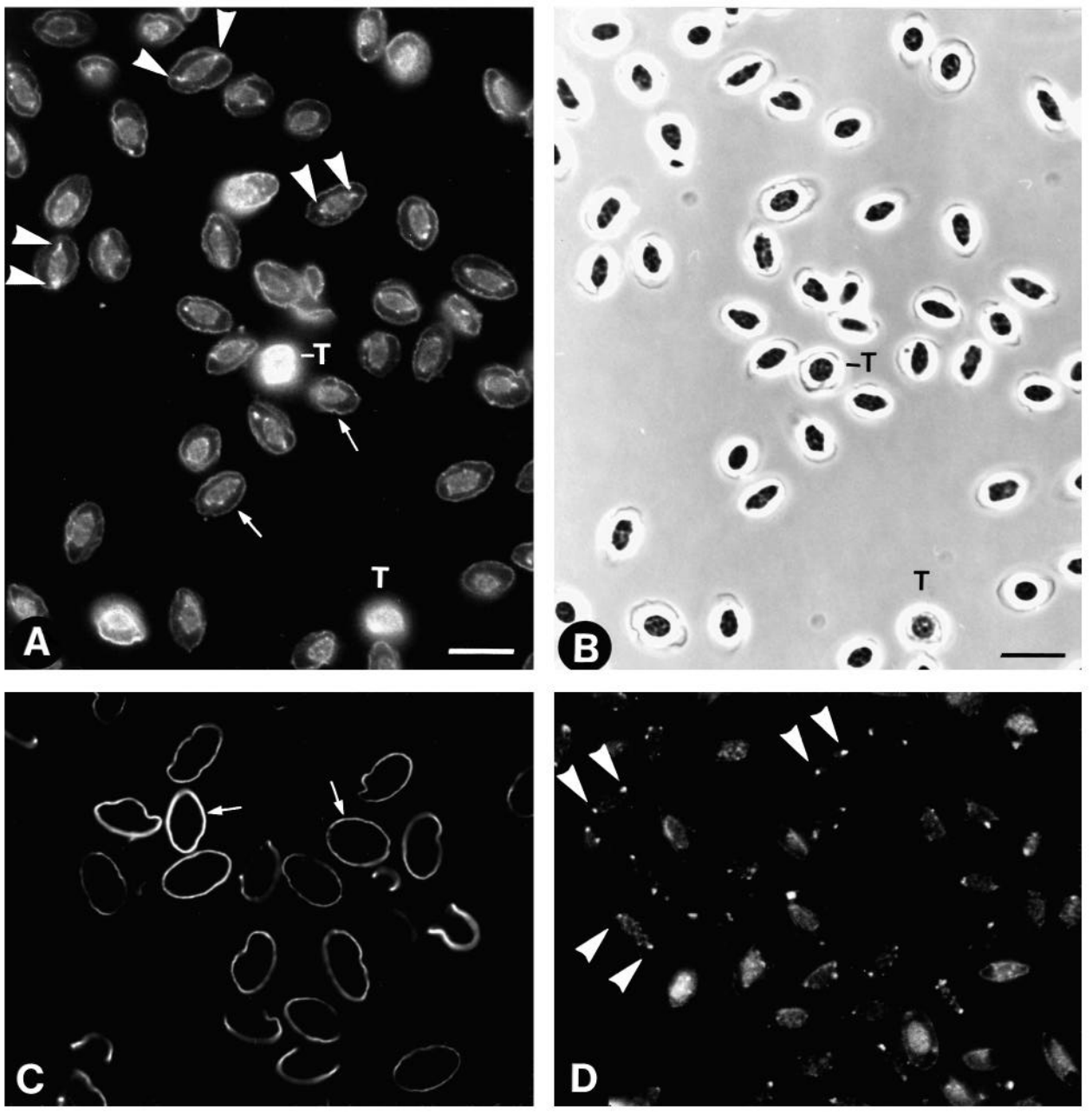

Fig. 4. Immunofluorescence localization of p23 in mature chick erythrocytes and thrombocytes. A represents immunostaining with anti-p23 mAb with the corresponding phase-contrast image in B. Both the MB (arrows) and centrosomes (seen as two dots shown by arrowheads on each side of the nucleus in most cells) were stained as well as the nuclear membrane. The MB p23 localization is confirmed by anti-tubulin staining (C) and the centrosomal localization by anti-human centrosome staining (D). The very bright cells were identified as thrombocytes (shown as T) on the basis of their morphology and tendancy to aggregate. Arrowheads indicate centrosomes. Bar, 10 μm.

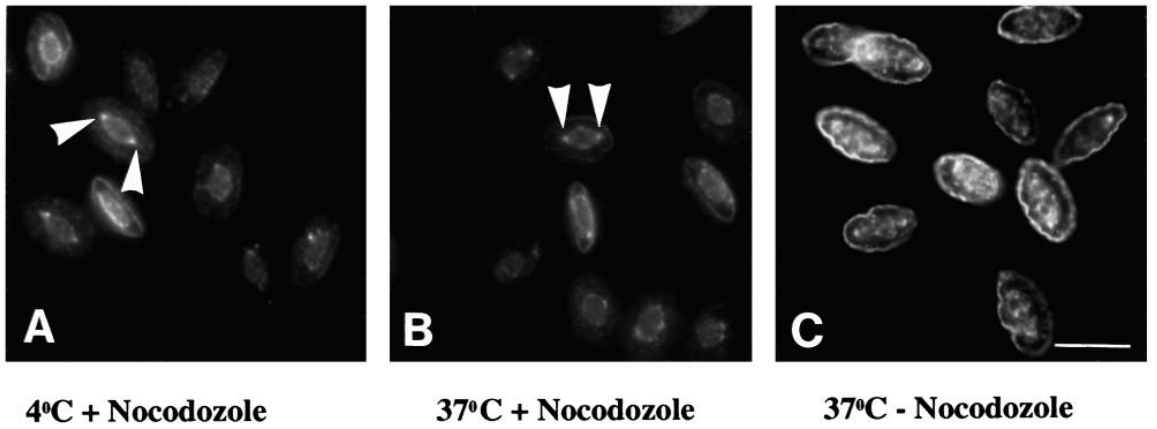

Fig. 5. Effect of MT destabilization on p23-MB localization. Mature chick erythrocytes were pretreated for 1 hour at 4°C prior to immunofluorescence staining with anti-p23 (A) or allowed to rewarm at 37°C for 30 minutes in the presence (B) or absence (C) of 5 μM nocodazole. Note that the MB but not centrosomal p23 staining is abolished by cold treatment. Arrowheads indicate centrosomes. Bar, 10 μm.

was now completely restored. However, in cells pre-exposed to 10^{-4} M $[Ca^{2+}]_{free}$, this effect could not be reversed either for p23 or MB MTs (data not shown), presumeably because of additional detrimental effects of the prolonged exposure of cells to these high cytosolic free Ca^{2+} levels such as activation of the Ca^{2+}-activated proteases.

Transfection and expression of chick p23

The centrosomal and MB localization of p23 in chick erythrocytes coupled with its Ca^{2+}-sensitivity led to the question of whether the lineage-restricted expression of p23 had any role to play in MB or centrosomal stability. To address the potential function of p23, p23 cDNA was subcloned into pCDNAI, PRC/RSV or pSVL and the resultant constructs transfected into COS or primary CEF cells. IF staining revealed that within the first 36 hours after transfection in both cell types, p23 was localized predominantly within the nucleus (Fig. 8A,B). Subsequently, p23 became diffusely localized throughout the cytoplasm (Fig. 8C,D). Identical results were obtained for all the constructs. No evidence was seen for any association with either the cytoplasmic or spindle arrays of MTs or with the centrosomes in these cells. Thus, p23 expression failed to recapitulate any of the p23 interactions observed in post-mitotic terminally differentiated erythrocytes in these mitotic, relatively undifferentiated cells and had no detectable effects on cell growth or morphology.

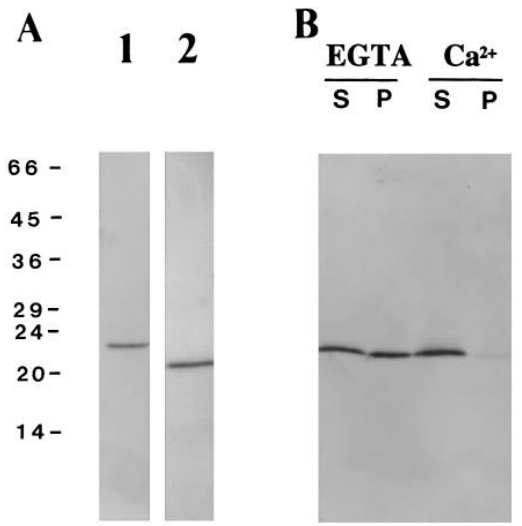

Fig. 6. Ca^{2+} effects on p23. (A) Direct effects of Ca^{2+} on p23 mobility in SDS-PAGE. Chick erythrocyte lysates were run under conditions of either 1 mM EGTA (lane 1) or 1 mM Ca^{2+} (lane 2) included in the sample buffer, 20% SDS-PAGE and running buffer. Molecular mass markers ($\times 10^{-3}$) run alongside each erythrocyte lane are designated. These all showed no shift in apparent M_r under either condition. (B) The effect of Ca^{2+} on p23 solubility; including EGTA (set 1) or 1 mM Ca^{2+} (set 2) in the hypotonic lysis buffer. S, the soluble fraction; P, the insoluble pellet.

p23 expression and localization during erythropoiesis

One possible explanation for the lack of any visible consequence of heterologous p23 expression is that there is a fundamental difference between the nature of the dynamic interphase MT arrays and MTOC functioning centrosomes in COS and CEF cells, and the highly stable MB MTs, and the inactive centrosomes/nonreplicating centrioles in differentiated erythrocytes and thrombocytes. Alternatively, the differences in the complement of MAPs or tubulin modifications between the different cell types might also affect the ability of p23 to interact with these structures in the transfected cells. In addition, MBs contain a unique β-tubulin variant, cβ6 (Murphy and Wallis, 1983a), so the possibility exists that p23 can only interact with erythroid-specific β-tubulin-containing MTs. To examine this further we analyzed the expression and localization of p23 as a function of erythropoiesis, using developing erythroblasts isolated at different stages of embryonic development, since the initial primitive and subsequent definitive erythrocyte lineage develop as a synchronized cohort in circulation in a well defined manner (Lucas and Jamroz, 1961; Bruns and Ingram, 1973).

Day 2 circulating primitive erythroblasts were found to be predominantly negative for both p23 and cβ6 β-tubulin (data not shown). A few circulating primitive cells (5-10%) in day 3 embryos, representing early polychromatophilic (PE) primitive

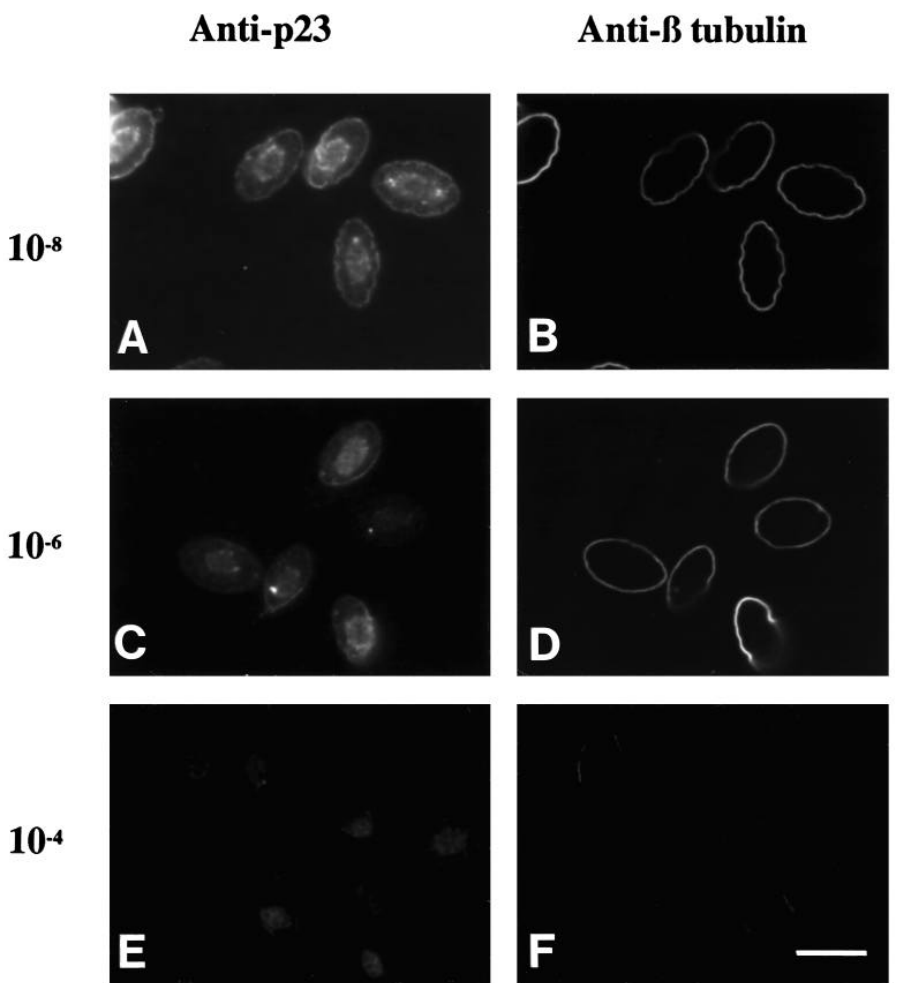

Fig. 7. IF of the effects of modulating intracellular $[Ca^{2+}]_{free}$ on anti-p23 and anti-tubulin staining. Cells were incubated in different Ca^{2+}/EGTA buffers in the presence of 1 μM A23187 prior to double IF with anti-p23 (A,C,E) or anti-tubulin (B,D,F). $[Ca^{2+}]$ of 10^{-8} M (A,B), 10^{-6} M (C,D) and 10^{-4} M (E,F) are shown. Bar, 10 μm.

erythroblasts, were now seen to stain positively for p23, which was distributed diffusely throughout the cytoplasm (Fig. 9A,B). A slightly higher percentage (≈25%) were found to be positive for cβ6 β-tubulin, which appeared predominantly in the form of quasi MB structures. Noticeably, the cβ6-positive cells appeared to have few, if any, individual cytoplasmic MTs although cβ6 antisera did stain the spindle apparatus of the occasional dividing cell (Fig. 9A,C). This indicates that cβ6-

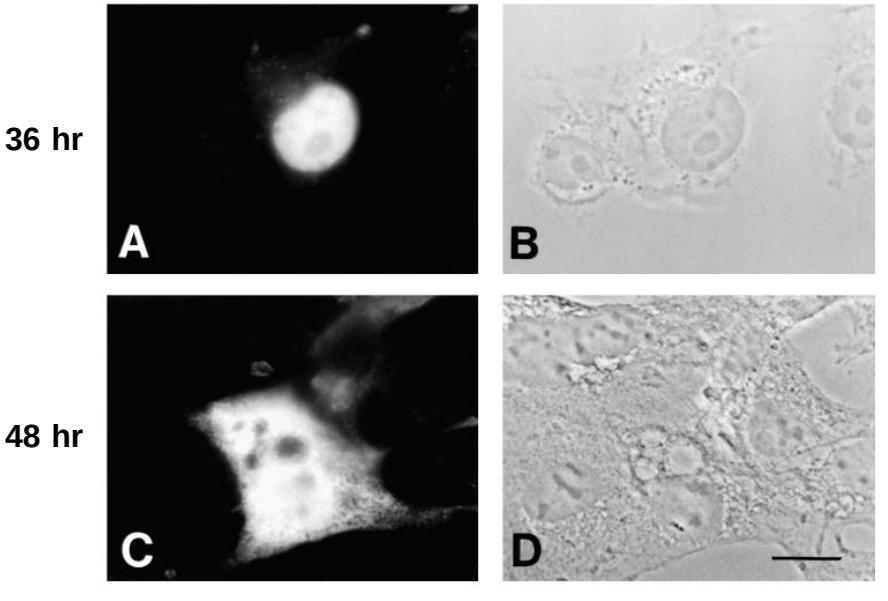

Fig. 8. IF of p23 localization following transient transfection of the p23 cDNA into COS cells. The fluorescent and corresponding phase-contrast images obtained 36 hours (A,B) and 48 hours (C,D) after transfection are shown. Bar, 20 μm.

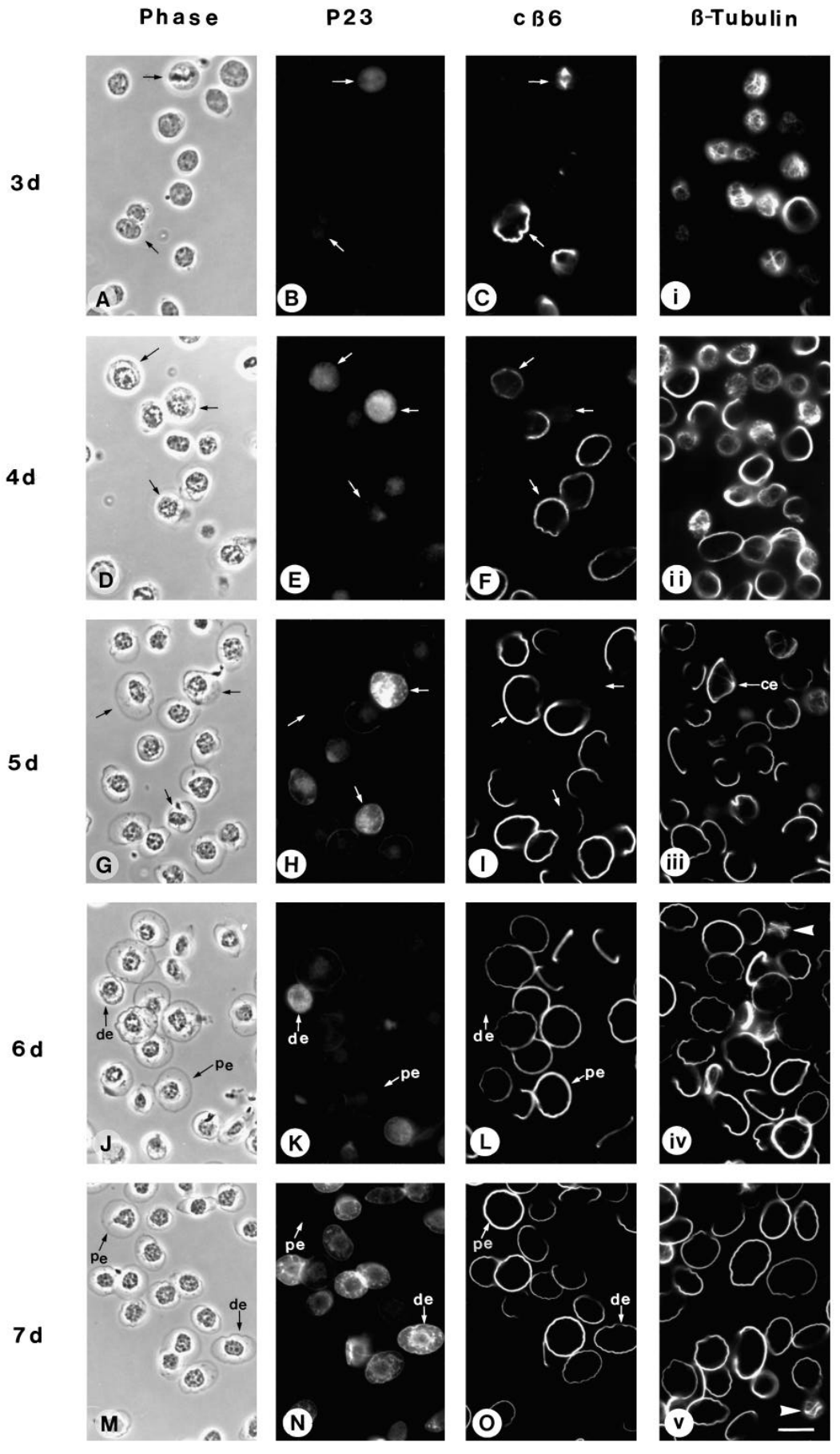

Fig. 9. p23-cytoskeletal associations during embryonic erythropoiesis. Double IF of p23 (B,E,H,K,N) and cβ6 β-tubulin (C,F,I,L,O) localization together with general β-tubulin localization (i,ii,iii,iv,v) in circulating erythrocytes isolated at the different days of embryonic development shown with the corresponding phase-contrast images. An active centrosome in an erythroid cell at 5 days is indicated by ce in iii; an early definitive erythroblast (de) at 6 days is compared with a primitive erythrocyte (pe) in J, K and L and at 7 days in M, N and O. Arrows in panels A-C, D-F and G-I highlight examples showing that p23-expression in the primitive lineage appears to be restricted to erythroblastic stages whereas primitive cells expressing mature MBs are p23-negative. Note the p23-positive mitotic cell in the upper portion of panels A-C where cβ-6-tubulin is found deployed in the mitotic spindle. Arrowhead in iv indicates MT bundles encircling the cell. Bar, 10 μm.

containing MTs can reorganize to generate a mitotic spindle. At this developmental stage, the quasi MBs tended to weave in and out of the plane of focus around the cell. Staining with the antibody recognizing all β-tubulin isoforms revealed that the majority of cells contained cytoplasmic arrays, with many cells already containing coils of MT bundles within the cell even prior to upregulation of cβ6 expression. Double IF with the two anti-β-tubulin antibodies confirmed that the few cells with quasi MBs corresponded to the cβ6-positive cells (data not shown). This indicates that MT bundling precedes cβ6 expression, but the appearance of cβ6-containing MTs coincides with the association of these MT bundles with the plasma membrane as a MB. By day 4, many of circulating erythroblasts (polychromatophilic stage) now stained positively for cβ6, which was almost exclusively assembled into consolidating MB structures juxtaposed to the plasma membrane (Fig. 8F). Those cells still expressing cytoplasmic arrays corresponded to the cβ6-negative cells (data not shown). As indicated in Fig. 9iii, an occasional cell was observed where staining with the general β-tubulin antibody revealed the presence of the MTOC/centrosome (indicated by the arrow marked ce). We also observed the same array at earlier stages. Careful searching of many cells showed that when such a centrosome was visible it always appeared to be quite distant from the developing MB, as shown in Fig. 9iii. It was also noteworthy that in cells expressing loosely coiled bundles encircling the cell, the presumed precursor to the equatorial tight band of the MB, no evidence could be found, using the general anti-β tubulin, for any associated MTOC. Thus, at least at this stage, the centrosome did not appear to direct the establishment of the MB. From day 6 onwards the primitive cells all expressed mature MBs, manifested as a flat peripheral circle in a single plane of focus. Although the number of p23-positive primitive erythroblasts increased from day 3, p23 remained diffusely localised throughout the maturation phase of the MB (Fig. 9E,G) and also failed to associate with the centrosomes even in fully mature postmitotic primitive erythrocytes.

Erythroblasts of the definitive lineage were first seen in circulation on day 6, readily distinguished from primitive erythroid cells by their morphology. All stained positively for p23 in a diffuse manner with noticably greater intensity than their primitive counterparts. The same cells were negative for cβ6 and from general β-tubulin staining were seen to lack MBs (Fig. 9J,K,L,iv). Although negative for cβ6, these definitive cells had distinct MT bundles in the cytoplasm that were not connected in any obvious fashion to a centrosomal structure, as observed in primitive erythroid cells. However, it is possible that such an association may have been obscured by the high local MT densities. By day 7, p23 now localized to the MB as well as granular patches coelescing around the nucleus in the definitive cells (about 50% of the total population, now at the late polychromatophilic stage: Fig. 9M,N,O). By this stage, the majority of definitive cells were cβ6-positive although the occasional negative cell was still observed. General β-tubulin staining showed that these cβ6-negative cells contained predominantly loose MT coils encircling the cell (see arrow, Fig. 9v). From day 8, when definitive erythroblasts are undergoing their final division, the major change was a gradual concentration of the granular perinuclear p23 staining around the nucleus, with progressively more cells adopting the double centrosomal/nuclear membrane localization, which is characteristic of mature erythrocytes, between days 11 and 14 as progressively more cells become postmitotic. IF of bone marrow smears confirmed that this developmental sequence of p23-cytoskeletal interactions also occurs in bone-marrow-derived erythroid cells in addition to clearly demonstrating that p23 is not expressed in any other hematopoietic cell type (J. Zhu, 1994).

p23 steady-state levels are determined by preferential stabilization during terminal differentiation

Since the IF studies revealed predominantly the cytoskeletal-bound fraction of p23, western and northern blot analyses were carried out to determine total transcript and protein steady-state levels as a function of erythroid development. As shown in Fig. 10, p23 protein levels are low in circulating primitive cells isolated from day 2 embryos but thereafter increase to a plateau at day 5. As the primitive lineage in circulation begins to be replaced from day 6-7 by the definitive erythroblasts, a dramatic increase in p23 protein steady-state levels occurs, plateauing at a maximal level at day 10. cβ6-Tubulin expression appears to lag behind p23 but cβ6 accumulates to a greater extent in the primitive lineage. There is a second peak in the total amount of cβ6-tubulin, the sharp rise correlating with the onset of definitive erythroblast release into the circulation, at day 7, declining to an intermediate plateau by day 10. This latter event coincides with the time the definitive cells begin to become postmitotic. Quantitative analysis of transcript levels from day 4 onwards indicates that cβ6 expression shows a biphasic curve corresponding to the overlapping curves for the two lineages. This correlates with the overall RNA levels,

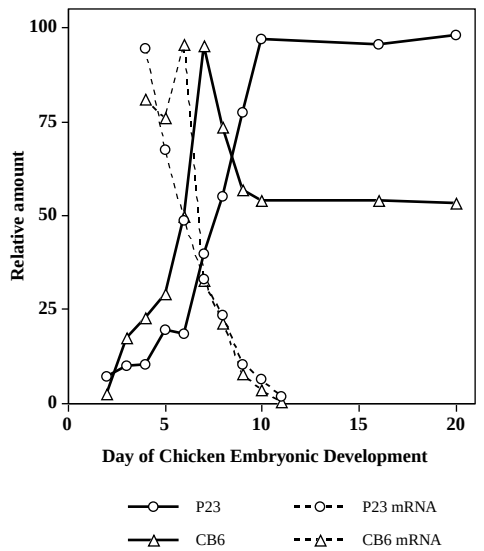

Fig. 10. Relative changes in p23 transcript and protein levels during development. Western and northern analysis were carried out with 10^5 and 5×10^6 cell equivalents, respectively, of circulating erythroid cells isolated at successive days of embryonic development. The same blots were probed for both p23 and cβ6 β-tubulin and the resulting signals scanned with a Molecular Dynamics densitometer and expressed in relative units. The data represent the values obtained from one experiment. Three independent experiments gave similar results.

which are high in the early erythroblastic stage and decline rapidly from day 9 (data not shown). p23 expression in contrast exhibits a steady decline, without showing a secondary peak around day 6-7 upon release of early definitive erythroblasts. Surprisingly, therefore, p23 expression is highest in early primitive cells despite the lack of any apparent p23-cytoskeletal interactions in these cells. Rather, cytoskeletal interactions are initiated specifically in definitive cells at a time when p23 expression is being markedly downregulated. Thus stabilization events resulting from p23-cytoskeletal interactions must dictate the overall accumulation of p23 protein at these late stages.

DISCUSSION

We have identified and characterized a novel Ca^{2+}-regulated protein in chick, p23, which lacks homology with any previously described polypeptide sequence. Its expression is lineage specific, being restricted to the erythrocyte and thrombocyte lineages. IF reveals that a fraction of p23 is associated in a Ca^{2+}-dependent manner with the MB, centrosomes and nuclear membrane of mature chick erythrocytes and thrombocytes. Additional studies have revealed that anti-p23 interacts with *Xenopus*, goldfish and human platelet MBs, suggesting a correlation between p23 expression and MB-containing cells (J. Zhu, 1994). The fact that p23 localization to the MB is dependent on the presence of an intact MT bundle is reminiscent of MAP activity. However, other than being a highly basic protein (pI~9.5), a characteristic common to MT binding domains (Goedert et al., 1991; Brandt and Lee, 1993) and a property that in itself is sufficient to confer MAP-like activity to diverse proteins (e.g. see Pirollet et al., 1989; Erikson and Voter, 1976; Multigner et al., 1992), p23 does not appear to function as a classical MAP. p23 failed to exhibit MT association in heterologous expression studies (Fig. 7) or to display any evidence of direct MT interactions with purified tubulin in vitro (J. Zhu, 1994). Furthermore, the sequence lacks any of the repeat structural motifs of the MT binding domain found in tau and MAP2 (Goedert et al., 1991; Brandt and Lee, 1993). Erythroid MBs are composed of a unique β-tubulin isoform, cβ6 tubulin, which is the most divergent β-tubulin isoform (Murphy and Wallis, 1983a; Murphy et al., 1987). However, the possibility that p23 may function as a β-specific MAP was discounted by in vitro studies with purified erythroid tubulin (J. Zhu, 1994).

p23 exhibits Ca^{2+} sensitivity

p23 subcellular localization is highly sensitive to modulation of intracellular Ca^{2+} levels. Normally, p23 exists in equilibrium between a soluble and a cytoskeletally bound pool. As the intracellular concentration is increased to 10^{-6} M, the cytoskeletally bound p23 fully dissociates from the MB, centrosome and nuclear membrane. In addition, p23 exhibits a gel shift in apparent M_r in the presence of Ca^{2+} (Fig. 5A, see also accompanying paper by Woods et al.), a diagnostic feature of direct Ca^{2+}-binding proteins (Burgess et al., 1980). However, sequence analysis indicated that p23 lacks any homology with the two known classes of Ca^{2+}-binding proteins. It contains neither the consensus sequence for the pair of helix-loop-helix structural motifs that constitute the binding site of the 'EF hand' family typified by calmodulin (Nakayama et al., 1992) nor the repeated consensus sequence contained in a conserved 70 amino acid stretch characteristic of the annexin family (Burgoyne and Geisow, 1989). To date we have been unable to unequivocally demonstrate direct $^{45}Ca^{2+}$-binding to p23 by equilibrium dialysis since we were unable to purify sufficiently high concentrations of native p23 that would be required for statistically significant binding data. Nevertheless, the data suggest that p23 may represent a novel Ca^{2+}-binding protein. Furthermore, p23 binding to its target skeletal binding sites requires low [Ca^{2+}], with concentrations of 10^{-6} M being sufficient to induce maximal p23 dissociation. Interestingly, this [Ca^{2+}] is not high enough to induce MB MT depolymerization. Although Ca^{2+} is known to disrupt MTs, in vitro this occurs at mM concentrations (Dustin, 1984); Ca^{2+}-induced MT depolymerization at physiological concentrations has been shown to be mediated by calmodulin (Marcum et al., 1978) and Ca^{2+}-induced MB dissociation involves non-calmodulin cytoplasmic factors (Gambino et al., 1985). These observations indicate that the Ca^{2+}-induced changes in p23 localization are unlikely to be mediated by calmodulin.

p23 and MB biogenesis

Detailed IF analysis of p23 association with the MB, centrosomes and nuclear membrane as a function of erythroid differentiation was undertaken to gain insight into the potential functional significance of these interactions. Considering first the temporal sequence in the elaboration of the MB, as also noted by others, we observed that a high degree of MT bundling occurs in the early polychromatophillic erythroblast stage of both primitive and definitive lineages, and precedes the association of an MB-like structure with the equatorial rim of the cell (Kim et al., 1987; Murphy et al., 1986). The MB-membrane association occurs coordinately with upregulation in the erythroid-specific β-tubulin during the late polychromatophilic stage (results described herein; Murphy et al., 1986). Throughout this time in both lineages p23 expression is high but p23 protein fails to accumulate and shows no evidence of any MB association. Since p23 fails to bind to the MB in mature primitive cells and MB association in definitive erythroid cells occurs after the bundled MTs have coalesced into a coherent, membrane-bound MB, p23 cannot be playing any readily apparent role in the biogenesis of the MB structure per se. We can only conclude that p23-MB interactions are induced specifically during the final maturation stages of definitive erythropoiesis. In addition, the onset of p23-cytoskeletal interactions results in a marked accumulation of p23 protein due to a pronounced stabilization against catabolism at a time when p23 biosynthesis is in rapid decline. This would be analogous to the mechanisms regulating the accumulation of the membrane skeleton during erythroid terminal differentiation (Lazarides, 1987). With this analogy in mind, one potential role for p23 may be to function as an ultimate MB stabilizing factor, similar to the manner protein 4.1 and ankyrin are incorporated into the membrane skeleton to crosslink the spectrin-actin network in the postmitotic stages of erythrocyte maturation (Lazarides, 1987).

p23 centrosomal interactions

p23 is also found associated with the erythrocyte and thrombocyte centrosomes and nuclear membrane. From the struc-

tural level analyzed in this study, it cannot be shown whether p23 is associated with the centriolar or PCM component of the erythrocyte centrosome. The size and Ca^{2+}-binding properties of p23 are reminiscent of the properties of caltractin/centrin (McFadden et al., 1987; Huang et al., 1988; Lee and Huang, 1993). However, structural sequence analysis revealed no homology between p23 and these proteins.

Analysis of p23-centrosomal interactions as a function of primitive and definitive erythroid differentiation failed to reveal any correlation between p23-centrosomal interactions with any specific stage of the centrosomal cycle in function. Thus p23-centrosomal interactions did not correlate per se with centrosomal MTOC interphase activity or the switch from directing interphase to spindle MT arrays in either lineage since p23 failed to interact with the centrosome in primitive or early definitive erythrblastic cycling cells despite high levels of p23 expression. Furthermore, they did not correlate with the inactivation of MTOC activity that occurs during erythrocyte terminal differentiation since no p23 cytoskeletal associations were observed in post-mitotic primitive erythrocytes. Rather, p23 centrosome/nuclear membrane localization is first visualized at day 7 as granular perinuclear staining specifically in the definitive lineage. This granular staining gradually coelesces around the nuclear membrane from day 8 onwards, assuming the double dot centrosomal and nuclear membrane localization characteristic of the mature erythrocyte as the cells become postmitotic. From day 7, classical centrosomally directed MTOC activity as the focal point of MT arrays are no longer observed. Although it cannot be ruled out that the local high MT densities in these small round erythroblast cells may have obscured such evidence, it has been noted that centrosomal antisera failed to demonstrate centrosomal links to the developing MB (Miller and Solomon, 1984) suggesting that MB MTs arise from membrane-localized MTOC activity (Kim et al., 1987). In other terminally differentiated cell types highly stable MT arrays are thought to arise from dispersed MT nucleating activity rather than from classical centrosomes (Tassin et al., 1985; Mogensen and Tucker, 1987; Baas and Ahmad, 1992). In such cases the PCM may become quite dispersed. In terminally differentiating erythrocytes the centriolar cycle becomes blocked at a stage after the centrioles have divided and assumed a position on either end of the nucleus (Searle and Bloom, 1979; Euteneuer et al., 1985; results described herein), a localization characteristic of early prophase. The PCM may encircle the nucleus prior to complete establishment of the spindle poles (Reider and Borisy, 1982; Mazia, 1987). Recent studies have indicated that some PCM components remain constitutively associated with the centrosome (Doxsey et al., 1994), but association of others, noticeably γ-tubulin and PCM-1, appears conditionally linked to centrosomal MTOC activity (Balczon et al., 1994; Félix et al., 1994; Stearns et al., 1994). The cell-cycle-induced pattern of PCM-1 localization after dissociation from the centrosome at the onset of mitosis is particularly interesting, being reminiscent of the granular perinuclear staining that we observed at days 7 and 8. Therefore, it is tempting to suggest that these anti-p23 reactive granular perinuclear aggregates that we observe at day 7 represent dispersed PCM material that has become inactive in MT nucleating activity, with the association being induced precisely at the time the centrosome becomes blocked from entering mitosis. If this indeed proves to be the case, the possibility exists that p23 is associating specifically with PCM material that has become inactive in MT nucleating activity specifically in definitive cells. This could also explain the lag between MB formation and p23-MB association if p23 is indeed interacting with MB-localized PCM components.

Ca^{2+} changes may regulate p23-cytoskeletal associations in erythroid development

Given that initiation of p23 interactions with quite disparate cytoskeletal structures occur coordinately at the same stage of erythroid development, these associations must be effected by some global change(s) occurring specifically in these late stages of definitive erythroid differentiation. Given the Ca^{2+}-sensitivity of p23-cytoskeletal interactions, it seems reasonable to speculate that changes in $[Ca^{2+}]_{free}$ might be a major determinant. One of the late events during the differentiation of nucleated definitive erythrocytes is the down-regulation/elimination of most intracellular organelles, analogous to the complete elimination of intracellular organelles that occurs in enucleate mammalian erythrocytes (Parmley, 1988; Searle and Bloom, 1979; Granger and Lazarides, 1982). Elimination of mitochondria and the ER should result in lower than normal $[Ca^{2+}]_{free}$ in erythrocytes. Indeed intracellular levels of 60 nM have been recorded in non-aged human erythrocytes (Aiken et al., 1992). With the improved methodology now available to measure intracellular $[Ca^{2+}]$ it should be possible to compare the resting free $[Ca^{2+}]$ in primitive and definitive erythroid cells. This would resolve the issue of whether the onset of p23 association with the erythroid cytoskeleton is induced simply by the lowering of intracellular Ca^{2+} levels during the final erythroid stages or whether additional factors specific to these late definitive stages are also required.

We thank Drs Douglas Murphy and William Brinkley for generously providing the anti-cβ6 and human centrosomal antibodies, respectively, Debbie Carlyle and Ping Ye for dedicated technical help, and Drs Thomas Coleman and Daniel Bollag for helpful discussions during the course of this work. The earlier part of this work was funded by a grant from the American Cancer Society to E.L. while at the California Institute of Technology.

REFERENCES

Aiken, N. R., Satterlee, J. D. and Galey, W. R. (1992). Measurement of intracellular Ca^{2+} in young and old human erythrocytes using F-NMR spectroscopy. *Biochim. Biophys. Acta* **1136**, 155-160.

Baas, P. W. and Ahmad, F. J. (1992). The plus ends of stable microtubules are the exclusive nucleating structures for microtubules in axons. *J. Cell Biol.* **116**, 1231-1241.

Baas, P. W. and Black, M. M. (1990). Individual microtubules in the axon consist of domains that differ both in composition and stability. *J. Cell Biol.* **11**, 495-509.

Balczon, R., Bao, L. and Zimmer, W. E. (1994). PCM-1, a 228-kD centrosome autoantigen with a distinct cell cycle distribution. *J. Cell Biol.* **124**, 783-793.

Barrett, L. A. and Dawson, R. B. (1974). Avian erythrocyte development: Microtubules and formation of the disk shape. *Dev. Biol.* **36**, 72-81.

Baum, P., Furling, C. and Byers, B. (1986). Yeast gene requried for spindle pole body duplication: homology of its product with Ca^{2+}-binding proteins. *Proc. Nat. Acad. Sci.* **83**, 5512-5516.

Behnke, O. (1970). A comparative study of microtubules of disk-shaped blood cells. *J. Ultrastruct. Res.* **31**, 61-75.

Birgbauer, E. and Solomon, F. (1989). A marginal band-associated protein has properties of both microtubule- and mircofilament-associated proteins. *J. Cell Biol.* **109**, 1609-1620.

Blikstadt, I. and Lazarides, E. (1983). Vimentin filaments are assembled from a soluble precursor in avian erythroid cells. *J. Cell Biol.* **96**, 1803-1808.
Brandt, R. and Lee, G. (1993). Functional organization of microtubule-associated protein tau. *J. Biol. Chem.* **268**, 3414-3419.
Bré, M., Pepperkok, R., Hill, A. M., Levilliers, N., Ansorge, W., Stelzer, E. H. K. and Karsenti, E. (1990). Regulation of microtubule dynamics and nucleation during polarization in MDCK II cells. *J. Cell Biol.* **111**, 3013-3021.
Brenner, S. L. and Brinkley, B. R. (1982). Tubulin assembly sites and the organization of microtubule arrays in mammalian cells. *Cold Spring Harbor Symp. Quant. Biol.* **46**, 241-254.
Brinkley, B. R. (1985). Microtubule organizing centers. *Annu. Rev. Cell Biol.* **1**, 145-172.
Bruns, G. A. and Ingram, V. M. (1973). The erythroid cells and haemoglobins of the chick embryo. *Philos. Trans. R. Soc. Lond. B. Biol. Sci.* **226**, 225-305.
Burgess, W. H., Jemiolo, d. K. and Kretsinger, R. H. (1980). Interaction of calcium and calmodulin in the presence of sodium dodecyle sulfate. *Biochim. Biophys. Acta* **623**, 257-270.
Burgoyne, R. D. and Geisow, M. J. (1989). The annexin family of calcium-binding proteins. *Cell Calcium* **10**, 1-10.
Cande, W. Z. (1980). A permeabilized cell model for studying cytokinesis using mammalian tissue culture cells. *J. Cell Biol.* **87**, 326-335.
Cassimeris, L. U., Pryer, N. K. and Salmon, E. D. (1988). Real-time observation of microtubule dynamic instability in living cells. *J. Cell Biol.* **107**, 2223-2231.
Cohen, W. D. (1978). Observations on the marginal band system of nucleated erythrocytes. *J. Cell Biol.* **78**, 260-273.
Doxsey, S. J., Stein, P., Evans, L., Calarco, P. D. and Kirschner, M. (1994). Pericentrin, a highly conserved centrosome protein involved in microtubule organization. *Cell* **76**, 639-650.
Dustin, P. (1984). *Microtubules*, 2nd edn. New York: Springer.
Erickson, H. P. and Voter, W. A. (1976). Polycation-induced assembly of purified tubulin. *Proc. Nat. Acad. Sci. USA* **73**, 2813-2817.
Euteneuer, U., Ris, H. and Borisy, G. G. (1985). Polarity of marginal band microtubules in vertebrate erythrocytes. *Eur. J. Cell Biol.* **37**, 149-155.
Feick, P., Foisner, R. and Wiche, G. (1991). Immunolocalization and molecular properties of a high molecular weight microtubule-bundling protein syncolin from chicken erythrocytes. *J. Cell Biol.* **112**, 689-700.
Félix, M., Antony, C., Wright, M. and Maro, B. (1994). Centrosome assembly in vitro: role of γ-tubulin recruitment in Xenopus sperm aster formation. *J. Cell Biol.* **124**, 19-31.
Gambino, J., Ross, M. J., Weatherbee, J. A., Gavin, R. H. and Eckhardt, R. A. (1985). Xenopus marginal band disassembly by calcium-activated cytoplasmic factors. *J. Cell Sci.* **79**, 199-216.
Goedert, M., Crowther, R. A. and Garner, C. C. (1991). Molecular characterization of microtubule-associated proteins tau and MAP2. *Trends Neurosci.* **14**, 193-199.
Gould, R. P. and Borisy, G. G. (1977). The pericentriolar material in Chinese hamster ovary cells nucleates microtubule formation. *J. Cell Biol.* **73**, 601-615.
Granger, B. L. and Lazarides, E. (1982). Structural association of synemin and vimentin filaments in avian erythrocytes revealed by immunoelectron microscopy. *Cell* **30**, 263-275.
Horio, T. and Hotani, H. (1986). Visualization of the dynamic instability of individual microtubules by dark-field microscopy. *Nature* **321**, 605-607.
Huang, B., Mengersen, A. and Lee, V. D. (1988). Molecular cloning of cDNA for caltractin, a basal body-associated Ca^{2+}-binding protein: homology in its protein sequence with calmodulin and the yeast CDC31 gene product. *J. Cell Biol.* **107**, 133-140.
Hughes, S. H., Greenhouse, J. J., Petropoulos, C. J. and Sutrave, P. (1987). Adaptor plasmids simplify the insertion of foreign DNA into helper-independent retroviral vectors. *J. Virol.* **61**, 3004-3012.
Joseph-Silverstein, J. and Cohen, W. D. (1984). The cytoskeletal system of nucleated erythrocytes. 3: marginal band function in mature cells. *J. Cell Biol.* **98**, 2118-2125.
Joshi, H. C., Palacios, M. J., McNamara, L. and Cleveland, D. W. (1992). γ-tubulin is a centrosomal protein required for cell cycle-dependent microtubule nucleation. *Nature* **356**, 80-83.
Kenney, D. M. and Linck, R. W. (1985). The cystoskeleton of unstimulated blood platelets: structure and composition of the isolated marginal microtubular band. *J. Cell Sci.* **78**, 1-22.
Kim, S., Magendantz, M., Katz, W. and Solomon, F. (1987). Development of a differentiated microtubule structure: formation of the chicken erythorcyte marginal band in vivo. *J. Cell Biol.* **104**, 51-59.
Kimble, M. and Kuriyama, R. (1992). Functional components of microtubule-organizing centers. *Int. Rev. Cytol.* **136**, 1-50.
Kirschner, M. and Mitchison, T. (1986). Beyond self-assembly: from microtubules to morphogenesis. *Cell* **45**, 329-342.
Kowit, J. D., Linck, R. W. and Kenney, D. M. (1988). Isolated cytoskeletons of human blood platelets: dark-field imaging of coiled and uncoiled microtubules. *Biol. Cell* **64**, 283-291.
Krestsinger, R. H. (1980). Structure and evolution of calcium-modulated proteins. *CRC Crit. Rev. Biochem.* **8**, 119-174.
Lazarides, E. (1987). From genes to structural morphogenesis: the genesis and epigenesis of a red blood cell. *Cell* **51**, 345-356.
Lee, V. D. and Huang, B. (1993). Molecular cloning and centrosomal localization of human caltractin. *Proc. Nat. Acad. Sci. USA* **90**, 11039-11043.
Loh, E. (1991). Anchored PCR: amplication with single-sided specificity. *Methods* **2**, 11-19.
Lucas, A. M. and Jamroz, C. (1961). *Atlas of Avian Hematology*. Agriculture monograph 25, US Department of Agriculture, Washington, DC.
Maniotis, A. and Schliwa, M. (1991). Microsurgical removal of centrosomes blocks cell reproduction and centriole generation in BSC-1 cells. *Cell* **67**, 495-504.
Marcum, J. M., Dedman, J. R., Brinkley, B. R. and Means, A. R. (1978). Control of microtubule assembly-disassembly by calcium-dependent regulator protein. *Proc. Nat. Acad. Sci. USA* **75**, 3771-3775.
Mazia, D. (1987). The chromosome cycle and the centrosome cycle in the mitotic cycle. *Int. Rev. Cytol.* **100**, 49-92.
McFadden, G. I., Schulze, D., Salisbury, J. L. and Melkonian, M. (1987). Basal body reorientation mediated by a Ca^{2+}-modulated contractile protein. *J. Cell Biol.* **105**, 903-912.
Miller, M. and Solomon, F. (1984). Kinetics and intermediates of peripheral determinants of microtubule organization. *J. Cell Biol.* **99**, 70-75.
Mitchison, T. and Krischner, M. (1984a). Microtubule assembly nucleated by isolated centrosomes. *Nature* **312**, 232-237.
Mitchison, T. and Krischner, M. (1984b). Dynamic instability of microtubule growth. *Nature* **312**, 237-242.
Mogensen, M. M. and Tucker, J. B. (1987). Evidence for microtubule nucleation at plasma membrane-associated sites in Drosophila. *J. Cell Biol.* **88**, 95-107.
Multigner, L., Gagnon, J., Dorsselaer, A. V. and Job, D. (1992). Stabilization of sea urchin flagellar microtubules by histone H1. *Nature* **360**, 33-39.
Murphy, D. B. and Wallis, K. T. (1983a). Brain and erythrocyte microtubules from chicken contain different β-tubulin polypeptides. *J. Biol. Chem.* **258**, 7870-7875.
Murphy, D. B. and Wallis, K. T. (1983b). Isolation of microtubule protein from chicken erythrocytes and determination of the critical concentration for tubulin polymerization in vitro and in vivo. *J. Biol. Chem.* **258**, 8357-8364.
Murphy, D. B. and Wallis, K. T. (1985). Erythrocyte microtubule assembly in vitro. *J. Biol. Chem.* **260**, 12293-12301.
Murphy, D. B. and Wallis, K. T. (1986). Erythrocyte microtubule assembly in vitro: tubulin oligomers limit the rate of microtubule self-assembly. *J. Biol. Chem.* **261**, 2319-2324.
Murphy, D. B., Grasser, W. A. and Wallis, K. T. (1986). Immunofluorescence examination of β-tubulin expression and marginal band formation in developing chicken erythroblasts. *J. Cell Biol.* **102**, 628-635.
Murphy, D. B., Wallis, K. T., Machlin, P. S., Ratrie III, H. and Cleveland, D. W. (1987). The sequence and expression of the divergent β-tubulin in chicken erythrocytes. *J. Biol. Chem.* **262**, 14305-14312.
Nakayama, S., Moncrief, N. D. and Kretsinger, R. H. (1992). Evolution of EF-hand calcium-modulated proteins. II. domains of several subfamilies have diverse evolutionary histories. *J. Mol. Evol.* **34**, 416-448.
Nelson, W. J. and Lazarides, E. (1983). Switching of subunit composition of muscle spectrin during myogenesis in vitro. *Nature* **304**, 364-368.
Oakley, C. E. and Oakley, B. R. (1989). Identification of γ-tubulin, a new member of the tubulin superfamily encoded by *mipA* gene of Aspergillus nidulans. *Nature* **338**, 662-664.
Oakley, B. R., Oakley, C. E., Yoon, Y. and Jung, M. K. (1990). γ-tubulin is a component of the spindle pole body that is essential for microtubule function in Aspergillus nidulans. *Cell* **61**, 1289-1301.
Olmsted, J. B. (1986). Microtubule-associated proteins. *Annu. Rev. Cell Biol.* **2**, 421-457.
Parmley, R. T. (1988). Mammals. In *Vertebrate Blood Cells* (ed. A. F. Rowley and Ratcliffe), pp 337-425. NA Cambridge University Press.
Pickett-Heaps, J. D. (1969). The evolution of the mitotic apparatus: An

attempt at comparative ultrastructural cytology in dividing plant cells. *Cytobios* **3**, 257-280.

Pirollet, F., Ranch, C. T., Joh, D. and Margolis, R. L. (1989). Monoclonal antibody to microtubule-associate STOP protein: affinity purification of neuronal STOP activity and comparison of antigen with activity in neuronal and nonneuronal cell extracts. *Biochemistry* **28**, 835-842.

Rieder, C. L. and Borisy, G. G. (1982). The centrosome cycle in PtK_2 cells: assymetric distribution and structural changes in pericentriolar material. *Biol. Cell* **44**, 117-132.

Reinsch, S. S., Mitchison, T. J. and Kirschner, M. (1991). Microtubule polymer assembly and transport during axonal elongation. *J. Cell Biol.* **115**, 365-379.

Sakai, H. and Ohta, H. (1991). Centrosome signalling at mitosis. *Cell Signalling* **3**, 267-272.

Schulze, E. and Kirschner, M. (1988). New feature of microtubule behaviour observed in vivo. *Nature* **334**, 356-359.

Searle, B. M. and Bloom, S. E. (1979). Influence of the bn gene on mitosis of immature red blood cells in turkeys. *J. Heredity* **70**, 155-160.

Spurling, N. W. (1981). Comparative physiology of blood clotting. *Comp. Biochem. Physiol.* **68**, 541-548.

Stearns, T., Evans, L. and Kirschner, M. (1994). In vitro reconstitution of centrosome assembly and function: the central role of γ-tubulin. *Cell* **76**, 623-637.

Stetzkowski-Marden, F., Deprette, C. and Cassoly, R. (1991). Identification of tubulin-binding proteins of the chicken erythrocyte plasma membrance skeleton which colocalize with the microtubular marginal band. *Eur. J. Cell Biol.* **54**, 102-109.

Swan, J. A. and Solomon, F. (1984). Reformation of the marginal band of avian erythrocytes in vitro using calf-brain tubulin: peripheral determinants of microtubule form. *J. Cell Biol.* **99**, 2108-2113.

Tassin, A., Maro, B. and Bornens, M. (1985). Fate of microtubule-organizing centers during myogenesis in vitro. *J. Cell Biol.* **100**, 35-46.

Tucker, J. B., Paton, C. C., Richardson, G. P., Morgensen, M. M. and Russel, I. J. (1992). A cell suface-associated centrosomal layer of microtubule-organizing material in the inner pillar cell of mouse cochlea. *J. Cell Biol.* **102**, 215-226.

Wacker, I. U., Rickard, J. E., Mey, J. R. D. and Kreis, T. E. (1992). Accumulation of a microtubule-binding protein, pp170, at desmosomal plaques. *J. Cell Biol.* **117**, 813-824.

Woods, C. M., Zhu, J., Coleman, T., Bloom, S. E. and Lazarides, E. (1995). Novel centrosomal protein reveals the presence of multiple centrosomes in turkey (*Meleagris gallopavo*) *bnbn* binucleated erythrocytes. *J. Cell Sci.* **108**, 000-000.

Zhu, J. (1994). Identification and characterization of a novel Ca^{2+}-binding protein in avian erythrocytes. Ph.D thesis, California Institute of Technology. (University Microfilm Inc.)

(Received 19 July 1994 - Accepted 6 October 1994)